OPTIMIZATION OF RADIO FREQUENCY HEATING OF IN-SHELL EGGS THROUGH FINITE ELEMENT MODELING AND EXPERIMENTAL TRIALS

S. R. S. Dev, S. Kannan, Y. Gariépy, and G. S. Vijaya Raghavan[*]

Department of Bioresource Engineering, McGill University, 21111 Lakeshore Road, Sainte Anne de Bellevue, Quebec H9X 3V9, Canada

Abstract—Considering Radio Frequency (RF) heating as a viable alternative for the in-shell heating of eggs, Finite Element Modeling and simulation of RF heating of in-shell eggs at 27.12 MHz were carried out to assess the feasibility and heating uniformity of the process. According to the recommendations of USDA-FSIS for the pasteurization of eggs, egg white must be heated up to 57.5°C, and the egg yolk has to be heated up to 61.1°C for 2 min. The objective of the simulation was to determine the location of hot and cold spots generated due to non-uniform heating. A parallel plate setup for Radio Frequency heating was simulated for different electric field strength levels and orientations of the egg (long axis parallel and long axis perpendicular to the plates). The simulation results were experimentally verified and the simulation procedure was validated using a laboratory parallel plate RF setup. A coaxial cavity design was simulated with a similar approach. Results indicated that both the parallel and coaxial cavity designs were suitable for in-shell pasteurization of eggs provided that the eggs were rotated to maintain the uniformity in heating. After the simulation of RF heating process, the process optimization was carried out to determine the most effective procedure for the process. The varying parameters obtained by using different modeling techniques for radiofrequency heating of in-shell eggs, were optimized using MATLAB. Laboratory scale experimental trials were conducted to test the validity and effectiveness of the optimized parameters. The optimal parameters set forth were found to be more efficient in terms of heating time and uniformity.

1. INTRODUCTION

Eggs are considered to be one of the natural complete meals available as they have all the essential amino acids [1]. In addition, eggs are one of the good sources of vitamins, minerals, folic acid and choline among many other micronutrients [2]. The unparalleled functional properties of the egg make it an essential ingredient in the food processing and baking industry. Unfortunately, there are various egg recipes which involve the use of uncooked raw eggs. Due to their high nutritional value, eggs are potential hosts of several bacteria notably *Salmonella enteritidis* (SE) [3]. SE is potent and efficient in successful invasion of the eggs that has led to several outbreaks of Salmonellosis (more than 90%) in the recent past, most of which has been traced back to the Grade A shell eggs [4, 5]. This calls for advanced safety protocols that regulate the safety of eggs. The present techniques for ensuring safety involves pasteurization of in-shell eggs primarily using hot water bath or steam, which are not effective, as they adversely affect the functional properties of the egg [6]. Due to this drawback, dielectric heating with the aid of Electro Magnetic Waves (EMW) like micro waves and radio waves are being evaluated to pasteurize the whole in-shell eggs [7].

Thermal processing of an egg is a direct approach. Though, measuring temperature at different points inside the shell is almost impossible due to the poor integrity and brittleness of the egg shell. Egg shell can host only a threshold level of holes after which egg shell breaks. However, it is mandatory to measure and analyze the temperature distribution inside the egg to evaluate the efficacy of the heating process. This type of analyses is essential as it will present the hot and cold spots inside the egg due to the heating process which could be optimized in such a way that the functional properties are least affected. As practical ways of determining the temperature distribution within a shell egg would be challenging and tedious, research for alternative ways of determining it is mandatory to design a good heating process for shell eggs. Recently, computer simulation studies have gained increased attention as they are increasingly used in studies to predict temperature distribution within biological medium in heating or cooking process [8–19]. For instance, Watanabe et al. have used computer simulation studies to predict the temperature distribution in frozen tuna when heated in commercial microwave oven [16]. The have coupled finite-difference time domain method, semi-implicit method, Monte Carlo method and radiative energy absorption distribution method to predict the temperature [16]. It was found that the predicted temperature by this method was well validated experimentally [16]. Birla et al. used finite

element computer modeling to predict the temperature distribution while heating a model fruit which is spherical in shape in parallel plate radio frequency (RF) heating system [8]. It was found that rotating the model fruit significantly increased the heating uniformity in the parallel plate RF heating system [8]. These studies suggest that such simulation techniques could be successfully employed to predict the temperature distribution of egg heated in RF applicator. Also, by fine tuning the parameters the process could be optimized to render desired temperature distribution within an egg so that the functional properties of the egg are preserved or least damaged.

Finite Element Method (FEM) had been employed successfully to solve complex partial differential equations which represent a non-homogenous, irregularly shaped system [12]. This study examines the suitability of FEM to predict the temperature distribution within shell eggs in parallel plate RF heating process and to further fine tune the process parameters to achieve the desired temperature distribution for uniform heating. Such uniform heating is essential to maintain the functional quality of the eggs. There are several parameters that are to be considered while designing the RF wave applicator to achieve uniformity in heating the eggs. For instance, orientation of electrodes, distance between the electrodes, geometry of the electrodes, length of the electrodes, spatial orientation of the egg between the electrodes and rotation of egg are few parameters that affects the uniform heating of eggs in RF heating system. With the optimized parameters FEM has been used to aid in the designing of the RF applicator with the desired parameters to render uniform heating [17]. Experimental verification of the optimized parameters is done subsequently with computer controlled parallel plate RF wave applicator (27.12 MHz) using an artificial glass eggs filled with egg white. Also, coaxial cavity method of RF heating was also simulated in a similar manner and the efficacies of the FEM in predicting the temperature distribution are compared.

2. MATERIALS AND METHODS

2.1. Mathematical Model

The problem of electromagnetic analysis on a macroscopic level is the problem of solving Maxwell's equations subject to certain boundary conditions. Maxwell's equations are a set of equations, written in differential form, as it leads to differential equations that the finite element method can handle. These equations state the relationships between the fundamental electromagnetic quantities. These quantities are the electric field intensity E and the magnetic field intensity H for

the corresponding dielectric properties of the medium.

2.2. Electromagnetics

The Maxwell's equations that govern the electromagnetic phenomena involving a given configuration resolved in 3D space are given by Equations (1)–(6) [20].

$$\frac{\partial E_x}{\partial t} = \frac{1}{\varepsilon_0 \varepsilon'} \left(\frac{\partial H_z}{\partial y} - \frac{\partial H_y}{\partial z} \right) - \frac{2\pi f \varepsilon''}{\varepsilon'} E_x \tag{1}$$

$$\frac{\partial E_y}{\partial t} = \frac{1}{\varepsilon_0 \varepsilon'} \left(\frac{\partial H_x}{\partial z} - \frac{\partial H_z}{\partial x} \right) - \frac{2\pi f \varepsilon''}{\varepsilon'} E_y \tag{2}$$

$$\frac{\partial E_z}{\partial t} = \frac{1}{\varepsilon_0 \varepsilon'} \left(\frac{\partial H_y}{\partial x} - \frac{\partial H_x}{\partial y} \right) - \frac{2\pi f \varepsilon''}{\varepsilon'} E_z \tag{3}$$

$$\frac{\partial H_x}{\partial t} = \frac{1}{\mu_0} \left(\frac{\partial E_y}{\partial z} - \frac{\partial E_z}{\partial y} \right) \tag{4}$$

$$\frac{\partial H_y}{\partial t} = \frac{1}{\mu_0} \left(\frac{\partial E_z}{\partial x} - \frac{\partial E_x}{\partial z} \right) \tag{5}$$

$$\frac{\partial H_z}{\partial t} = \frac{1}{\mu_0} \left(\frac{\partial E_x}{\partial y} - \frac{\partial E_y}{\partial x} \right) \tag{6}$$

The dynamically changing dielectric constant and loss factor were calculated using Equations (7)–(10) below as described in Kannan et al. [21].

$$\varepsilon'(EW) = \left(71.2 - 0.12\,T + 0.0004T^2 \right) e^{\frac{(4.84 + 0.03T)}{f}} \tag{7}$$

$$\varepsilon'(EY) = \left(21.53 + 6.36T - 0.0435T^2 + 0.010T^3 - 0.00008T^4 \right)$$
$$e^{\frac{(13.73 - 1.40T + 0.086T^2 - 0.0019T^3 + 0.00001T^4)}{f}} \tag{8}$$

$$\varepsilon''(EW) = 6.18 - 0.00026T - 0.00024T^2 + \frac{\left(12349.8 + 60.57T + 0.54T^2 \right)}{f} \tag{9}$$

$$\varepsilon''(EY) = 10.57 + 8.30T - 0.535T^2 + 0.012T^3 - 0.00095T^4$$
$$+ \frac{\left(12.83 - 1.28T + 0.07T^2 - 0.0018T^3 + 0.000013T^4 \right)}{f} \tag{10}$$

where,

EW — Egg White,

EY — Egg Yolk,

f — Frequency and,
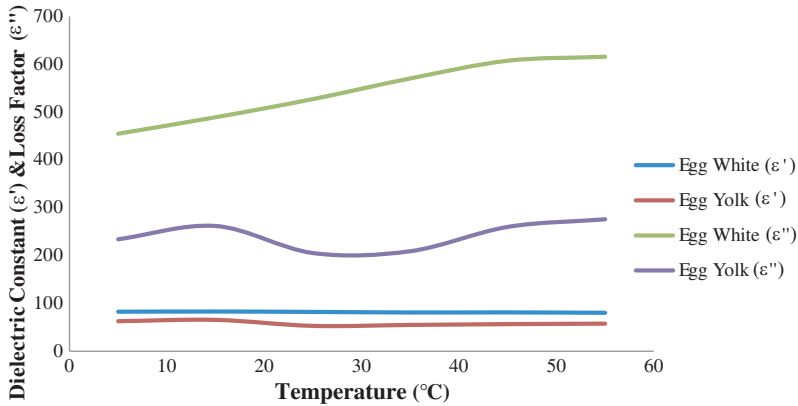
T — Temperature.

Figure 1. Variation of dielectric properties of egg white and egg yolk with temperature at 27.12 MHz.

Figure 1 shows the variation of the dielectric properties of egg white and egg yolk with temperature at 27.12 MHz [21] computed using Equations (7)–(10). Constant values of 5.0 and 0.5 were taken for the ε' and ε'' values of both the shell and shell membrane [7].

The time average electric field strength dissipated in each element in a dielectric material was obtained by integrating the Pointing vector over the closed surface S for each tetrahedral element [12]:

$$P_{av} = \frac{1}{2} \int_S P_c \cdot dS \tag{11}$$

where

$$P_c = E \times H$$

Volumetric heat generation can be expressed in terms of electric field strength intensity in three orthogonal directions [18]:

$$Q = \frac{\partial P_{av(x)}}{\partial V} + \frac{\partial P_{av(y)}}{\partial V} + \frac{\partial P_{av(z)}}{\partial V} \tag{12}$$

2.3. Boundary Conditions

Perfect Electrical Conductor boundary conditions ($n \times E = 0$) were used for the walls of the cavity and Perfect Magnetic Conductor boundary condition ($n \times H = 0$) was used for the symmetry boundaries [19].

Boundary conditions at the port were as follows:

$$H_y = A \cos\left(\frac{\pi x}{a}\right) \cos(\omega t + \beta y) \tag{13}$$

$$E_z = \left(\omega\mu_0\frac{a}{\pi}\right) A \sin\left(\frac{\pi x}{a}\right) \sin(\omega t + \beta y) \tag{14}$$

$$H_x = \left(\frac{\beta a}{\pi}\right) A \sin\left(\frac{\pi x}{a}\right) \sin(\omega t + \beta y) \tag{15}$$

2.4. Heat transfer

For an incompressible food material heated under constant pressure [19], the thermal energy equation is given by Equation (16).

$$\rho C_p \frac{\partial T}{\partial t} = \nabla \cdot (K\nabla T) + Q \tag{16}$$

3. SIMULATION

A Finite Element Model was developed using COMSOL Multiphysics version 3.4 (COMSOL Inc., USA) software package to simulate a parallel plate setup for Radio Frequency heating simulation at different electric filed strengths. This was achieved by operating the electrodes (60 mm apart) at 4.2, 5.0 and 5.7 kV. The parameters tested are the orientations of the egg (long axis parallel and long axis perpendicular to the plates). Also a simulation for a coaxial cavity design was carried out. Figure 2 shows the flow diagram of the simulation technique.

The general constitutive relationships (Equations (1)–(6)) get a little more complicated for a non-homogeneous material like eggs, as it requires interfacial boundary conditions. An non-homogeneous medium is one where the constitutive parameters vary with the space coordinates, so that different field properties prevail at different parts of the material structure. Therefore, a time domain based iterative solver was used which iteratively solves for the electromagnetic equations and the heat transfer equations for each time step. The time steps were chosen to be linear or logarithmic in real-time, adaptive to the convergence of the solution. This approach coupled with the bilateral symmetry of the cavity and waveguide was taken advantage in the simulations, thereby greatly reducing the resources required for running these simulations.

Considering a statistical accuracy of 95% in reality, for the simulations, any change less than 5% in the dielectric properties was considered statistically insignificant and therefore ignored. This helped performing the simulation like a step function wherein the electric field strength distribution was calculated only for every 5% change in dielectric properties, reducing the number of iterations by nearly 5 orders of magnitude, while still being able to account for transient dielectric properties.
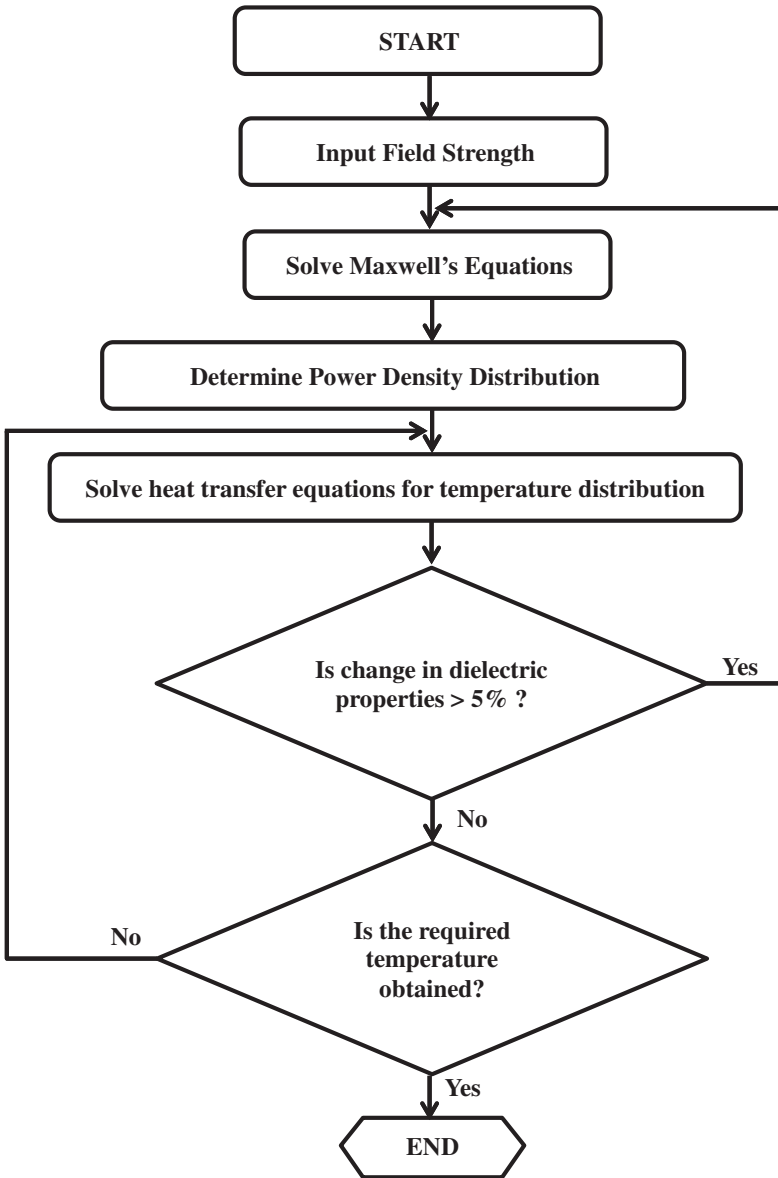
Figure 2. Flow diagram of FEM simulation technique.

Different element sizes were used for different sub-domains based on the dielectric properties of the sub-domain and the precision required in the sub-domain of interest. Also egg rotation was simulated by moving meshes with an angular velocity of $\frac{\pi}{18}$ rad·s^{-1}, programmed

using COMSOL Script version 1.2. Different configurations of RF
applicators like a parallel plate applicator and a coaxial cavity
applicator were simulated. Figures 3 and 4 give the FEM structure
of the cavities with parallel plate applicator and a coaxial waveguide
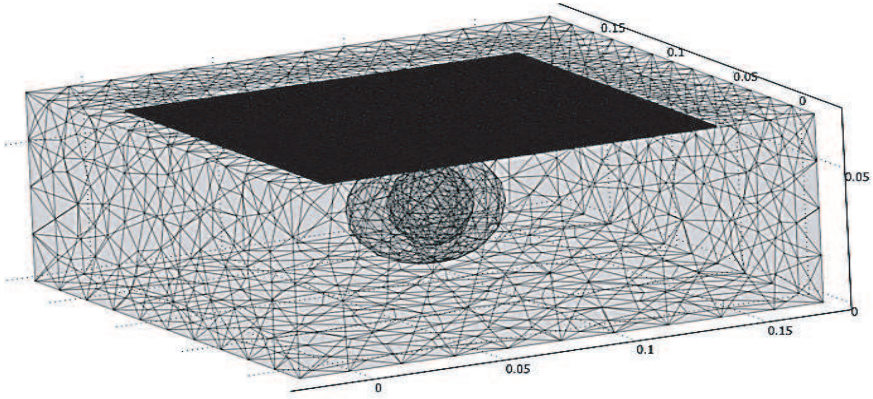applicator respectively.

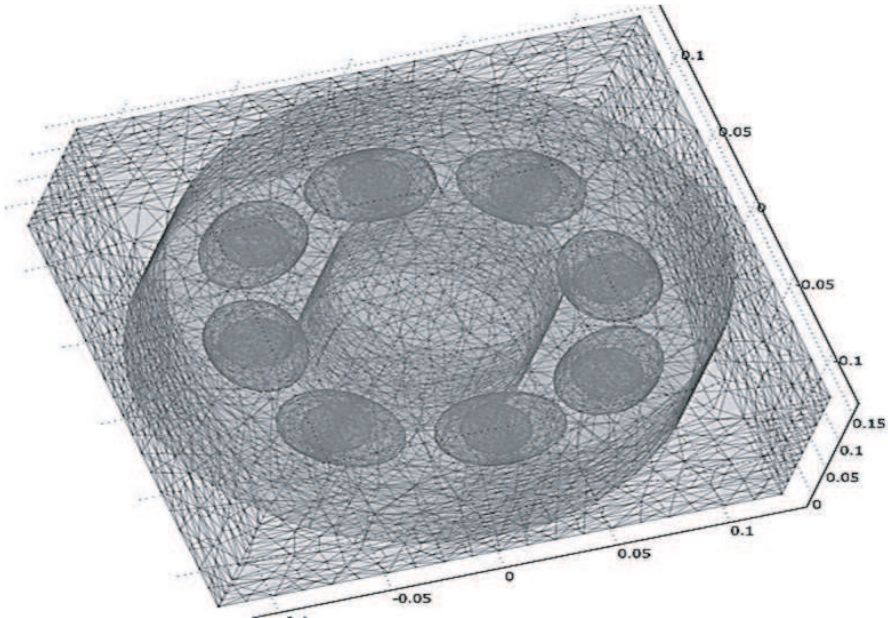**Figure 3.** FEM structure of the parallel plate applicator.

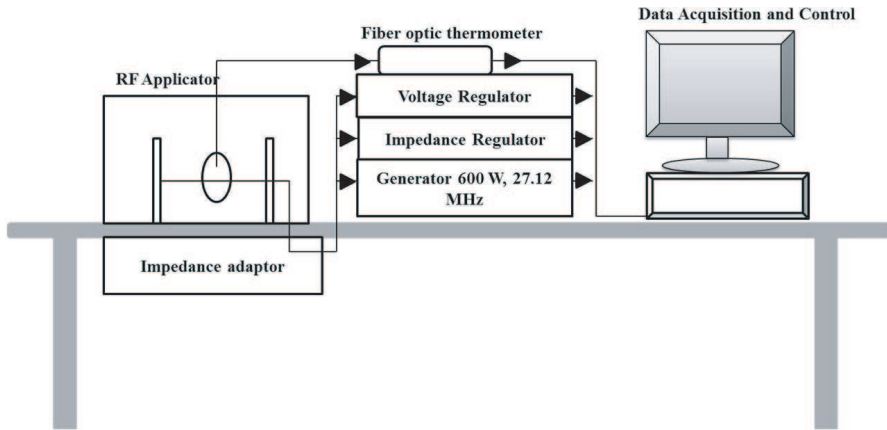**Figure 4.** FEM structure of the coaxial cavity applicator.

Figure 5. Schematic view of RF system.

A custom-built computer with Intel Core 2 Quad 2.4 GHz processor and 8 GB primary memory was used to run the simulations.

3.1. Experimental Validation

3.1.1. Equipment

Simulations were also computed for an all-white egg in order to be able to verify the simulation approach with an artificial egg (a transparent glass egg made with 40 ml of real egg white as shown in Figure 11). The simulation results were experimentally verified by heating the artificial egg in a custom built, computer controlled parallel plate RF applicator (Figure 5). The generator operates at a frequency of 27.12 MHz and has an impedance of 50 ohm and a maximum power output of 600 W for a maximum applied voltage of around 5 kV. The aluminum applicator plates are separated from each other by 60 mm. The RF generator was a circuit made of free running oscillator whose oscillations are sustained by a triode valve. The two galvanometers indicate the incident and reflected electric field strength. To maximize the energy transfer between the electric field strength source and the applicator, there should be equal impedance offered by the applicator and the generator. This is maintained by the automatic impedance adaptor between the generator and the applicator. This further aids in maximizing the power transfer at the same time minimizing the reflected power.

3.2. Experimental Design and Procedure

The temperature was recorded by the fiber optic probe that was introduced through the cap of the glass eggs. The experiment was repeated at different electric field strength densities. The electrodes are operated at voltages 4.2, 5.0 and 5.7 kV and the electrodes are 60 mm apart. Any non-uniformity in heating was not investigated. The artificial eggs were held at the temperature (56 ± 0.5°C) for 2.5 min. All the measurements were made in triplicates.

4. RESULTS

4.1. Simulation

It is clearly evident from the Figure 6 that heating in a parallel plate RF applicator (distance between the electrode is 5 mm) is highly non-uniform and this may lead to the generation of cold spots and hot spots
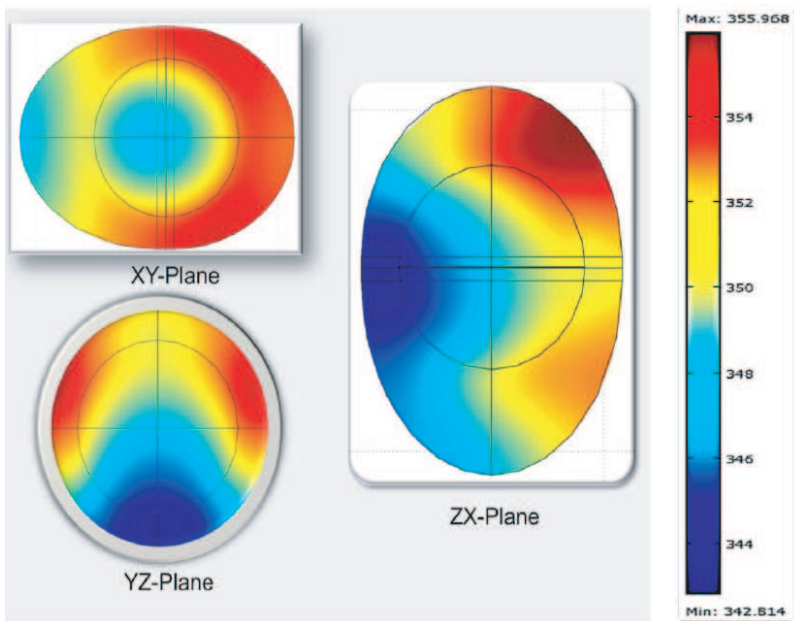

Figure 6. The simulation result of the temperature distribution in the in-shell egg in three different planes XY, YZ, ZX when heated in a parallel plate RF applicator with 5 mm air gap between the eggs and the electrodes. The eggs are kept static between the electrodes. The legend shows the temperature in K.

within the shell eggs. Clearly, egg white gets heated up faster than the egg yolk in the parallel plate RF applicator which is not desirable to sustain the functional properties of the egg.

The non-uniformity in heating is greater when the air gap between the egg and electrodes is reduced to 0.5 mm from 5 mm (Figure 7). The closer the eggs get to electrodes, faster the egg white gets heated up as compared to the egg yolk. It might lead to the increased coagulation
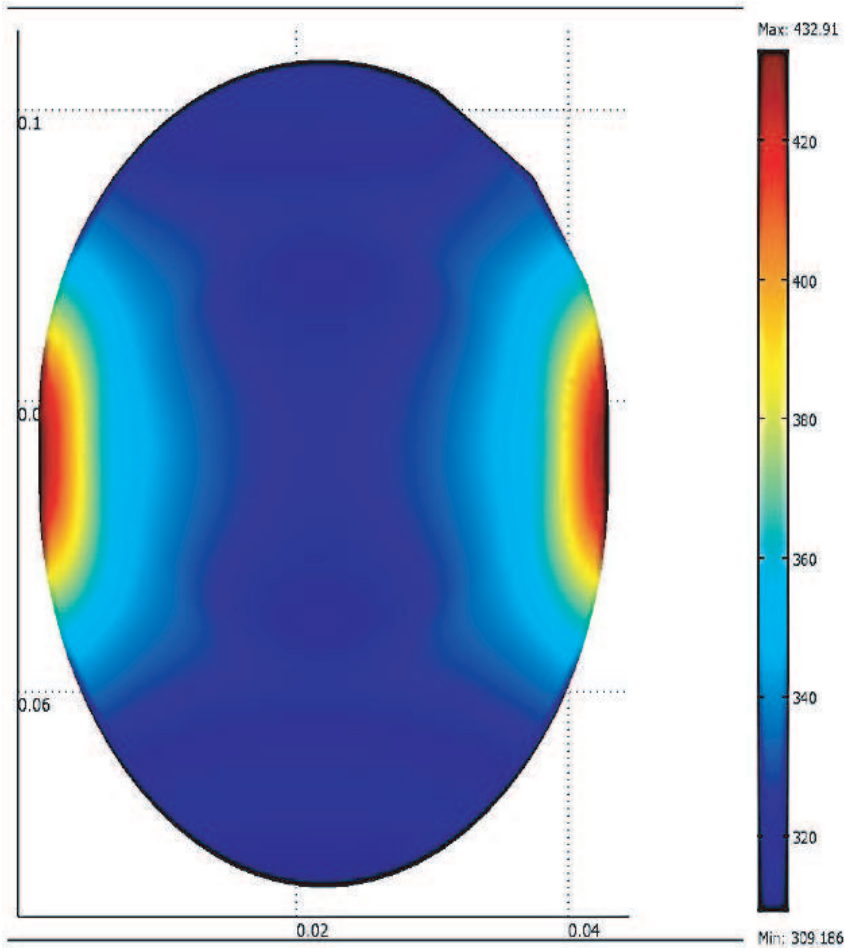

Figure 7. The simulation result of the temperature distribution of the in-shell egg heated in a parallel plate RF applicator with 0.5 mm air gap between the eggs and the electrodes. The eggs are kept static between the electrodes. The legend shows the temperature in K.
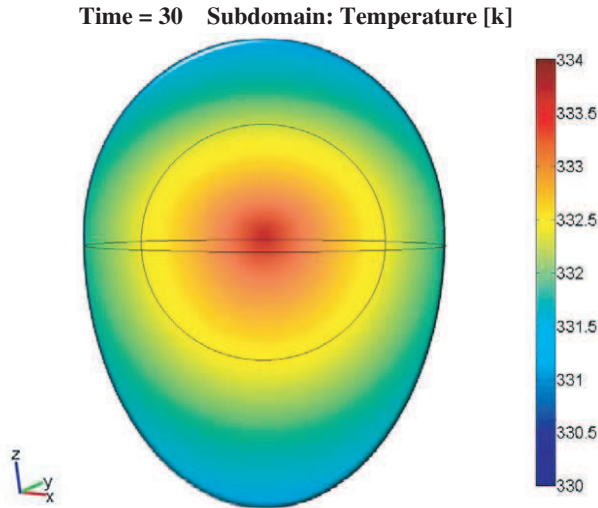
Time = 30   Subdomain: Temperature [k]

Figure 8. The simulation for the temperature distribution of the eggs heated in a parallel plate RF applicator with 5 mm air gap between the eggs and the electrodes. The eggs are rotated between the electrodes. The legend shows the temperature in K.

of the egg white proteins which is a major drawback as the functional properties of the egg will be severely affected.

On comparing the Figures 6, 7 (where the eggs were held static between the electrodes) and 8 (where the eggs were rotated between the electrodes), the temperature distribution of the eggs that are rotated seem to be convincingly uniform. The egg yolk is heated more than the egg white as preferred. This would be of great advantage for in-shell egg pasteurization process where heating the egg yolk more than the egg white is essential. Also as the heating is uniform, there will be no coagulation of the proteins in the egg white thereby maintaining the unique functional properties of the egg even after the heat treatment.

As it can be clearly seen from the Figure 9 that the inside of the coaxial cavity has low voltage and the outside of the cavity has higher voltage. When the eggs are kept static and heated in the coaxial cavity RF applicator, the temperature distribution in the in-shell egg is similar to that of the eggs when heated in a parallel plate RF applicator with 5 mm air gap (Figures 6 and 10). The only difference between the temperatures distributions of the two treatments observed is that there is a swap over between the temperature distribution in XY plane and the ZX plane. This is because the eggs are kept in a position where the heating takes place from top to bottom in the parallel plate RF applicator whereas in the coaxial cavity the heating takes place from side to side. This is a 90° switch in the direction of the heat application
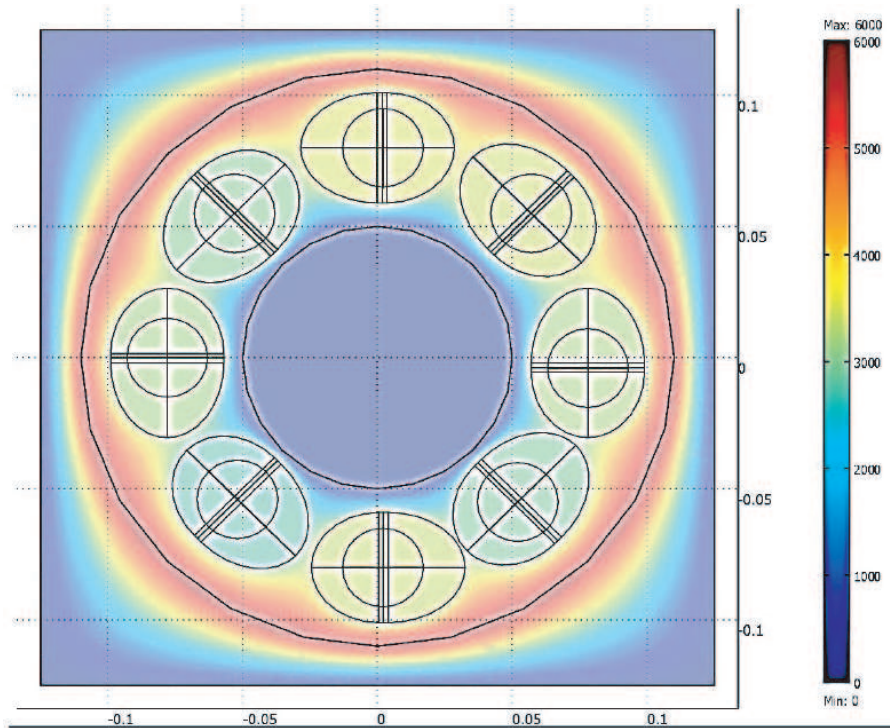
Figure 9. The simulation results of the electric field distribution in a coaxial cavity RF applicator when the eggs are heated. Eggs are kept static. The legend shows electric field in V/m.

between the two treatments and this has led to the switch over of the distribution patterns between the XY and ZX planes. In conclusion, when the eggs are kept static and heated in the coaxial cavity RF applicator, the heating is highly non uniform as in parallel plate RF applicator.

The simulation of the RF heating in a coaxial cavity RF applicator when the eggs are rotated and heated is very tedious and practically cumbersome. This is because the eggs are constantly fed into the RF applicator and at a time there are multiple eggs to simulate. So there is a need for a lot more resources and the process has numerous mathematical and numerical issues. We expect that by heating the eggs that rotate within a Teflon cylinder in a coaxial cavity RF applicator with 5 mm air gap between the electrodes and the eggs, it is possible to achieve more heating of the yolk than the white as the uniformity in the heating is maintained. This set up would be suitable for applications at an industrial scale.
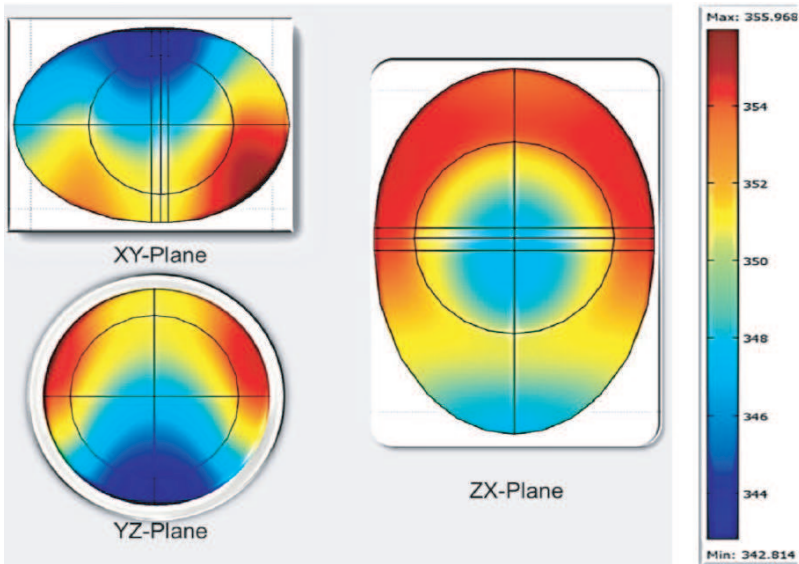
Figure 10. The simulation results of the temperature distribution in a coaxial cavity RF applicator when the eggs are heated. The eggs are kept static. The legend shows temperature in K.

4.2. Experimental Validation

Numerically simulated results corroborated well with the experimental data. The extent of coagulation obtained in the simulation and in the experiment (eggs are kept static and heated in a parallel plate RF applicator with 5 mm air gap) was in agreement. The Figure 11 shows the levels of coagulation observed upon heating egg white in specially designed glass eggs. It is clear from the picture that the extent of coagulation depends on the electric field strength level used (Figure 12). As the electric field strength level increased, the extent of coagulation also increased. As the egg white is heated the protein is denatured and loses its 3D confirmation which leads to a decrease in the density, as a result of which the coagulation lumps float to the top and forms a cooked layer at the top (indicated by red colored arrows in Figure 11).

By plotting the time taken to reach the desired temperature against the applied RF electric field (mean electric voltage/distance between the electrodes) in a parallel plate RF applicator, come up time (time taken for attaining a said temperature) and the heating rate is determined for the artificial glass eggs. The come up time and heating rate in a parallel plate RF applicator is given by the Equations (17) and (18) respectively (Figure 13). By using this equation, the come
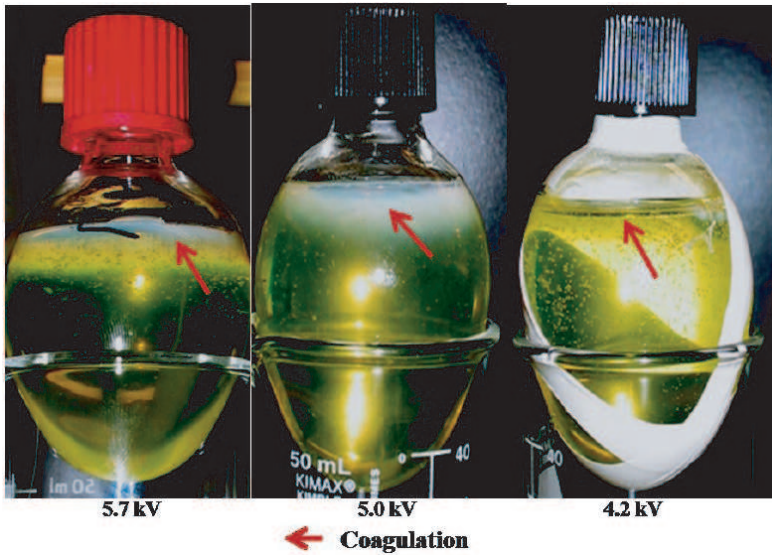
Figure 11. Experimental verification of the optimized simulation results.
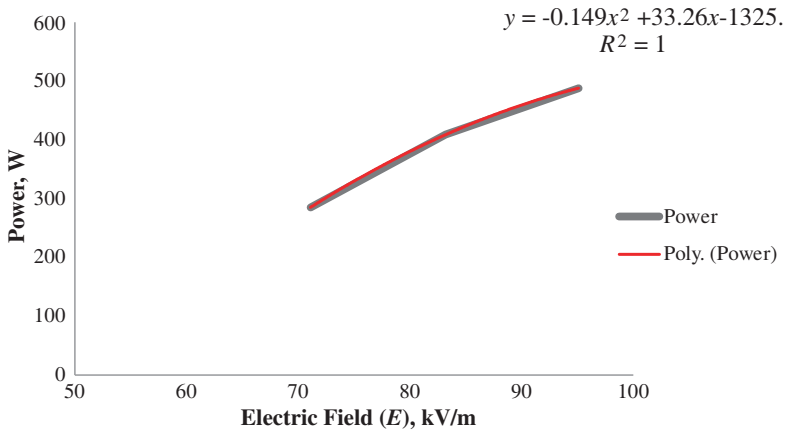

Figure 12. Relationship between the electric field of the RF and the Power generated.

up time and the heating rate could be predicted for any given electric field intensity for a parallel RF applicator.

$$H_T = 0.0029E^2 - 0.802E + 55.344\,\text{min} \tag{17}$$

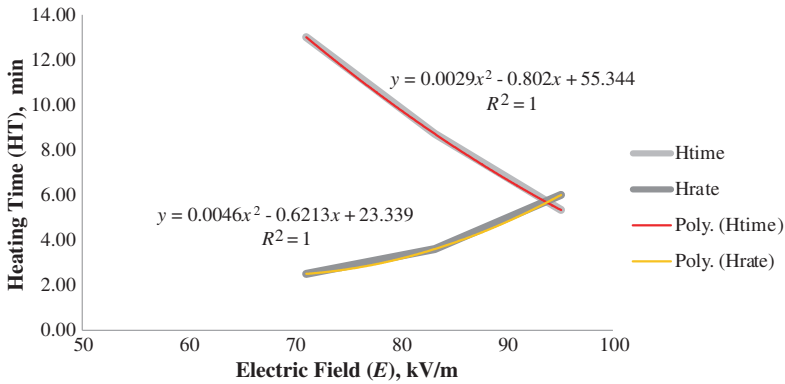$$H_R = 0.0046E^2 - 0.6213E + 23.339\,^{\circ}\text{C/min} \tag{18}$$

Figure 13. Heating time and rate of the parallel plate RF heated artificial Eggs.

5. DISCUSSION

The prediction of temperature distribution of egg while heating is essential to determine the adverse effects that the process might pose to the functional properties of the egg. Computer guided simulation techniques was adapted in this study as practical determination of the temperature distribution in a shell egg is quite challenging. The previous studies have shown that such simulation methods are quite accurate in predicting the temperature distribution in biological medium. In this study, FEM study was conducted to predict and fine tune the temperature distribution within the egg when it is heated in two different types of RF applicator (i) Parallel plate and (ii) Coaxial cavity. Different parameters (distance between the egg and electrode and orientation of the egg between the electrodes) were fine tuned to optimize the process to achieve uniform heating.

The results obtained showed that in a parallel plate RF applicator, when the eggs are kept static therein non uniformity in heating that might lead to hot and cold spots within the egg which is undesirable (Figure 6). This is due to that the region of egg that is in close proximity to the electrode heats faster than the region that is farther away. This is further confirmed when the non-uniformity in heating increased upon decreasing the air gap between the egg and electrode from 5 to 0.5 mm (Figures 6 and 7). This non-uniformity in heating was convincingly decreased when the eggs were rotated between the electrodes (comparing Figures 6, 7 and 8). As the egg rotates, different region of the eggs are in close proximity to the electrodes at different times. This leads to more uniformity in heating. In the coaxial cavity design RF applicator similar non uniform heating was observed

when the eggs are kept static. The only difference in the temperature distribution between the coaxial and parallel plate design was the swap over of the XY and ZX planes in coaxial design (Figures 9 and 10). This is due to the difference in the direction of heating of the eggs in the two configurations (Parallel — top to bottom and Coaxial — side to side).

The experimental validation of the simulated results showed that FEM could be used successfully to predict the temperature distribution of the eggs in a parallel plate RF applicator. When the eggs are kept static and heated in parallel plate RF applicator, non-uniformity in heating led to accumulation of cooked egg white at the top of the artificial glass eggs and is directly proportional to the electric field intensity (Figures 11 and 12). The hot spots might have led to coagulation of the proteins due to denaturation at different regions in the artificial egg. As the coagulated protein has less density, it floats to the top and forms a layer of cooked egg white. We have also derived equation for predicting the H_T and H_R for a given electric field intensity in a parallel plate RF applicator (Figure 13; Equations (17) and (18)).

6. CONCLUSION

This study aimed at evaluating the suitability of RF heating for in-shell eggs by conducting a FEM and simulation of the RF heating process. Two types of RF applicators namely parallel plate RF applicator and co-axial cavity design were simulated and it was found that both the process would be suitable for RF heating of in-shell eggs provided that the eggs are rotated in the applicator. Further experimental validation with laboratory scale parallel plate RF applicator showed that when eggs were kept static and heated it lead to coagulation of the egg white. This was due to non-uniformity in heating which partially cooks the egg white. This result validated the simulation results obtained from FEM. Thus, this study shows that FEM could be employed in predicting the temperature distribution within the egg in heating process and the parameters could be tweaked to optimize the process to uniformly heat the eggs. This optimized FEM parameters could ultimately be used to design the appropriate RF applicator to heat the in-shell eggs with minimal or no damage to the functional properties of the egg.

ACKNOWLEDGMENT

Nomenclature

E Total Electric field intensity (V m^{-1}).
E_x Electric field intensity x component (V m^{-1}).
E_y Electric field intensity y component (V m^{-1}).
E_z Electric field intensity z component (V m^{-1}).
H Total Magnetic Field Intensity (A m^{-1}).
H_x Magnetic field intensity x component (A m^{-1}).
H_y Magnetic field intensity y component (A m^{-1}).
H_z Magnetic field intensity z component (A m^{-1}).
F Frequency of microwaves (Hz).
ε' Dielectric constant.
ε'' Dielectric loss factor.
ε_0 Permitivity of free space (F m^{-1}).
μ_0 Permeability of free space (H m^{-1}).
P_{av} Time average power dissipated (W).
P_c Poynting Vector — power dissipated over unit area (W m^{-2}).
ρ Density of the material (kg m^{-3}).
C_p Specific heat capacity of the material (kJ kg^{-1} $^\circ$K^{-1}).
T Temperature ($^\circ$K).
T_c Temperature ($^\circ$C).
K Thermal conductivity (W m^{-2} $^\circ$K^{-1}).
Q Power Source Term (W m^{-3}).
V Volume (m^3).
n Unit vector normal to the surface.
A Cross sectional area of the waveguide.
α Length of the long side of the rectangular waveguide.
β Phase constant.
H_T Come up time (min).
H_R Heating rate ($^\circ$C/min).

REFERENCES

1. Swendseid, M. E., R. J. Feeley, C. L. Harris, and S. G. Tuttle, "Egg protein as a source of the essential amino acids: Requirement for nitrogen balance in young adults studied at two levels of nitrogen intake," *The Journal of Nutrition*, Vol. 68, 203–211, 1959.
2. Li-Chan, E. C. Y., W. D. Powrie, and S. Nakai, "The

chemistry of eggs and egg products," *Egg Science and Technology*, W. J. Stadelman and O. J. Cotterill (eds.), Food Products Press, New York, 1995.

3. FSIS-USDA, "Risk assessments for Salmonella enteritidis in shell eggs and Salmonella spp," *Egg Products*, FSIS, Omaha, 2006.

4. Schroeder, C. M., A. L. Naugle, W. D. Schlosser, A. T. Hogue, F. J. Angulo, J. S. Rose, E. D. Ebel, W. T. Disney, K. G. Holt, and D. P. Goldman, "Estimate of illnesses from Salmonella enteritidis in eggs, United States 2000," *Emerg. Infect. Dis.*, Vol. 11, 113–115, 2005.

5. Stlouis, M. E., D. L. Morse, M. E. Potter, T. M. Demelfi, J. J. Guzewich, R. V. Tauxe, and P. A. Blake, "The emergence of grade-a eggs as a major source of Salmonella-enteritidis infections — New implications for the control of salmonellosis," *Journal of the American Medical Association*, Vol. 259, 2103–2107, 1988.

6. Hou, H., R. K. Singh, P. M. Muriana, and W. J. Stadelman, "Pasteurization of intact shell eggs," *Food Microbiol*, Vol. 13, 93–101, 1996.

7. Dev, S. R. S., G. S. V. Raghavan, and Y. Gariepy, "Dielectric properties of egg components and microwave heating for in-shell pasteurization of eggs," *Journal of Food Engineering*, Vol. 86, 207–214, 2008.

8. Birla, S. L., S. Wang, and J. Tang, "Computer simulation of radio frequency heating of model fruit immersed in water," *Journal of Food Engineering*, Vol. 84, 270–280, 2008.

9. Campanone, L. A., C. A. Paola, and R. H. Mascheroni, "Modeling and simulation of microwave heating of foods under different process schedules," *Food and Bioprocess Technology*, Vol. 5, 738–749, 2012.

10. Campanone, L. A. and N. E. Zaritzky, "Mathematical modeling and simulation of microwave thawing of large solid foods under different operating conditions," *Food and Bioprocess Technology*, Vol. 3, 813–825, 2010.

11. Chen, H., J. Tang, and F. Liu, "Simulation model for moving food packages in microwave heating processes using conformal FDTD method," *Journal of Food Engineering*, Vol. 88, 294–305, 2008.

12. Jia, X. and P. Jolly, "Simulation of microwave field and power distribution in a cavity by a 3-dimensional finite-element method," *J. Microwave Power and Electromag Energy*, Vol. 27, 11–22, 1992.

13. Liu, C. M., Q. Z. Wang, and N. Sakai, "Power and temperature distribution during microwave thawing, simulated by using

Maxwell's equations and Lambert's law," *International Journal of Food Science and Technology*, Vol. 40, 9–21, 2005.

14. Olivera, D. F. and V. O. Salvadori, "Finite element modeling of food cooking," *Lat. Am. Appl. Res.*, Vol. 38, 377–383, 2008.

15. Tiwari, G., S. Wang, J. Tang, and S. L. Birla, "Computer simulation model development and validation for radio frequency (RF) heating of dry food materials," *Journal of Food Engineering*, Vol. 105, 48–55, 2011.

16. Watanabe, S., M. Karakawa, and O. Hashimoto, "Computer simulation of temperature distribution of frozen material heated in a microwave oven," *IEEE Trans. on Microw. and Theory*, Vol. 58, 1196–1204, 2010.

17. Zhou, L., V. M. Puri, R. C. Anantheswaran, and G. Yeh, "Finite-element modeling of heat and mass-transfer in food materials during microwave-heating — Model development and validation," *Journal of Food Engineering*, Vol. 25, 509–529, 1995.

18. Lin, Y. E., R. C. Anantheswaran, and V. M. Puri, "Modeling temperature distribution during microwave heating," *American Society of Agricultural Engineers*, Paper No. 89-6506, ASAE AIM, Saint Joseph, MI, USA, 1989.

19. Fu, W. and A. Metaxas, "Numerical prediction of three-dimensional power density distribution in a multimode cavity," *J. Microwave Power and Electromag Energy*, Vol. 29, No. 2, 67–75, 1994.

20. Dai, J., "Microwave-assisted extraction and synthesis studies and the scale-up study with the aid Of FDTD simulation," Dissertation, Department of Bioresource Engineering, McGill University, Canada, 2006.

21. Kannan, S., "Preliminary analyses of the dielectric properties of egg for radio frequency pasteurization," *NABEC*, Paper No. 11-020, Vol. 22, No. 1, Vermont, USA, 2011.